

Osteoporosis-specific Bone Mineral Crystallinity and Estrogen-Deficiency alter Mineralization in a 3D Mineralized Model

Mostafa Khabooshani¹, Syeda M. Naqvi¹, Stanislas Von Euw², Laoise M. McNamara¹

¹Mechanobiology and Medical Device Research Group, Biomedical Engineering, University of Galway, Ireland.

²School of biological and Chemical sciences, University of Galway, Ireland.

m.khabooshani1@universityofgalway.ie

INTRODUCTION: Our studies have shown that osteoporosis is not only a disease associated with bone loss, but that bone tissue composition and bone cell mechanobiology are fundamentally altered at the onset of estrogen deficiency [1-4]. In particular, osteoblasts and osteocytes exhibit changes in differentiation and mineralization when subjected to mechanical stimulation under estrogen deficiency [4]. However, our previous studies were conducted in 2D culture and a simplified 3D in vitro model, neither of which represent the highly mineralized mature bone, which exhibits a distinct hydrated surface amorphous calcium phosphate layer and a crystalline hydroxyapatite core [5]. Moreover, bone mineral composition, crystallinity and changes in the relative proportion of these layers have been identified in osteoporotic bone [5-7]. However, the influence of bone crystallinity of osteocyte differentiation and mineralization in estrogen deficiency is not yet fully understood. Here we (1) develop an advanced 3D model mimicking healthy and osteoporotic mineralized bone matrix and (2) investigate how osteoporosis-induced changes in bone crystallinity influence osteogenic differentiation and mineralization under estrogen deficiency.

METHODS: Novel synthetic bone-like proxies were created using platelet-shaped carbonated hydroxyapatite nanoparticles (nHA) coated with different proportions of hydrated amorphous surface layer (HASL), representing healthy (HE: 35%) and osteoporotic (OS: 20%) bone mineral. These healthy and osteoporotic nHA proxies were then incorporated into gelatin hydrogels at different relative concentrations (50%, 25% or 12.5% w/w). Osteoblasts (MC3T3-E1) were pre-treated with 17 β -Estradiol for 4 days and then encapsulated within these gelatin-nHA hydrogels (10⁶ cells/ml) and cross-linked with 1% wt mtgase. Subsequently, these constructs were cultured for 21 days in media supplemented with or without estrogen as follows: (1) continued estrogen and healthy mineral proxy (E, HE), (2) estrogen withdrawal and healthy proxy (EW, HE), (3) continued estrogen and osteoporotic mineral proxy (E, OS), and (4) estrogen withdrawal and osteoporotic proxy (EW, OS). TEM, XRD, SSNMR, biochemical assays (DNA, ALP, and calcium content), histological staining (DMP1/actin, Von-Kossa), mechanical testing and micro-CT scanning were conducted to determine the extent of osteogenic differentiation and mineralization.

RESULTS: Nano HA characterization: TEM (Fig. 1A), XRD and SSNMR results confirmed the formation of platelet nanosized calcium phosphate particles, involving HSAL and a crystalline HA core, for both healthy and osteoporotic bone mineral proxies. Crystallinity in HE and OS proxies were 65 % and 80 % respectively. **Cell proliferation and differentiation:** Within the 50% nHA-gelatin hydrogels, DNA analysis indicated significant proliferation for all groups by day 21, when compared to day 0, but no differences were observed between groups (Fig. 1F). Actin staining and SEM imaging revealed that the encapsulated cells exhibited a spherical morphology at day 0 (Fig. 1B, C). Morphological changes indicative of osteocyte differentiation (dendrite formation) were observed for all groups by day 21 (~100 μ m from the hydrogel surfaces) (Fig. 1B, C), and positive DMP1 staining was confirmed (Fig. 1D). **Osteogenesis and mineralization:** A significant reduction in ALP activity was reported under EW for both HE and OS groups by day 21 (Fig. 1G). There was no significant difference in calcium content under EW and E conditions for both OS and HE constructs (Fig. 1H). Both OS and HE constructs exhibited higher compressive stiffness and mineral deposition by day 21 compared to day 0 (Fig. 1I, E, J). In OS constructs the compressive stiffness and mineral deposition were significantly higher under estrogen withdrawal (EW) treatment compared to the E group. This trend was similarly noted in the HE groups, but was not statistically significant (Fig. 1I, E, J). Furthermore, stiffness and mineral deposition were higher in the OS compared to HE constructs under EW conditions. Mineral deposition was significantly higher in OS constructs compared to HE under E, but there was no significant difference in stiffness (Fig. 1I, E, J).

DISCUSSION: Here we created advanced 3D mineralized bone-like models to mimic the bone mineral structure of healthy and osteoporotic bone. We applied these to examine how estrogen deficiency influences differentiation and mineralization of bone cells. Similar to our previous studies, conducted in 2D culture and 3D [4], we report higher mineral deposition in EW groups. Here, we report for the first time that mineral deposition was higher when cells were cultured within the osteoporotic bone mineral proxy, which provided more nucleation sites for calcium and phosphate ions. Thus, the increase in crystallinity and reduction in water content on the HA surface might facilitate formation of hydroxyapatite crystals. Osteoblasts may detect the presence of variable mineral crystallinity in the osteoporotic condition, and their drive to ossify the environment varies accordingly [8]. Further studies will uncover the underlying mechanisms underpinning changes in mineralization in estrogen deficiency and arising due to changes in crystallinity.

SIGNIFICANCE/CLINICAL RELEVANCE: This advanced model mimics the complex *in vivo* mineral microenvironment of bone tissue during postmenopausal osteoporosis. We report that osteoporosis-specific bone mineral crystallinity and estrogen-deficiency alter osteogenic mineralization.

REFERENCES: [1] Brennan et al, J Mech Behav Biomed Mater, 29:161, 2014. [2] Simfia et al, Exp Cell Res, 392(1):112005, 2020. [3] Geoghegan et al, Sci Rep, 9(1):1, 2019. [4] Naqvi et al, Front Bioeng Biotechnol, 8:601, 2020. [5] Zeng et al, ACS Biomater Sci and Eng, 7.3: 1159-1168, 2021. [6] Gamsjaeger, Acta Biomaterialia, 124, 2021, [7] Brennan, Calcified Tissue International, 91(6), 2012, [8] Uskoković et al, ACS Biomater Sci and Eng, 5:7, 2019.

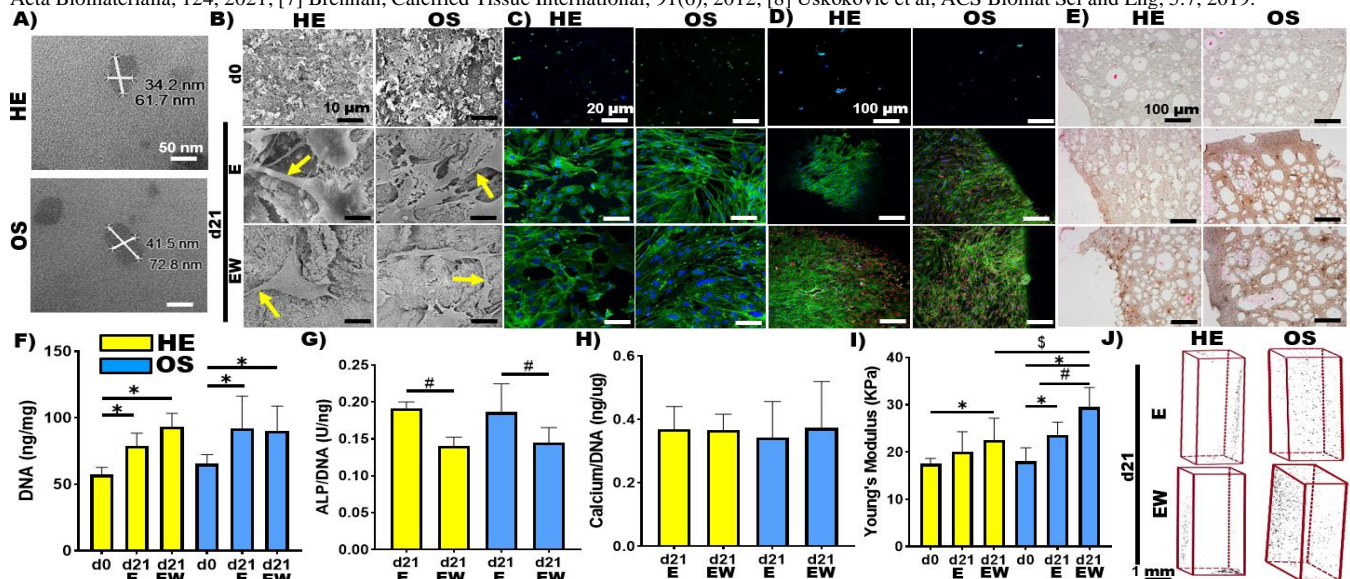


Figure 1: (A) TEM images for HE and OS proxies, (B) SEM images for the 50% nHA-gelatin hydrogels HE and OS constructs, yellow arrows indicate dendritic cells, (C) Actin (green) and DAPI (blue) staining ~100 μ m from the hydrogel surfaces, (D) Actin (green), DMP1 (red) and DAPI (blue) staining, (E) Von Kossa staining, (F) DNA content, (G) ALP activity, (H) Calcium content, (I) compressive stiffness for OS and HE constructs, (J) Micro-CT 3D reconstruction. Significant differences ($p < 0.05$) indicated relative to earlier time points (*), continuous estrogen (#), and Healthy (\$).